Journal of Power Sources 195 (2010) 3345–3358

Contents lists available at ScienceDirect

Journal of Power Sources

journal homepage: www.elsevier.com/locate/jpowsour

Review

Oxygen reduction and transportation mechanisms in solid oxide fuel cell cathodes

Yihong Li[a,b], Randall Gemmen[a], Xingbo Liu[a,b,*]

[a] National Energy Technology Laboratory, Morgantown, WV 26507, USA
[b] Mechanical & Aerospace Engineering Department, West Virginia University, Morgantown, WV 26506, USA

ARTICLE INFO

Article history:
Received 8 November 2009
Received in revised form
13 December 2009
Accepted 14 December 2009
Available online 22 December 2009

Keywords:
Solid oxide fuel cells
Cathode modeling
Kinetics

ABSTRACT

In recent years, various models have been developed for describing the reaction mechanisms in solid oxide fuel cell (SOFC) especially for the cathode electrode. However, many fundamental issues regarding the transport of oxygen and electrode kinetics have not been fully understood. This review tried to summarize the present status of the SOFC cathode modeling efforts, and associated experimental approaches on this topic. In addition, unsolved problems and possible future research directions for SOFC cathode kinetics had been discussed.

Contents

* Corresponding author at: Mechanical & Aerospace Engineering Department, West Virginia University, P.O. Box 6106, Morgantown, WV 26506, USA. Tel.: +1 304 293 3111x2324; fax: +1 304 293 6689.
E-mail address: xingbo.liu@mail.wvu.edu (X. Liu).

0378-7753/$ – see front matter © 2009 Elsevier B.V. All rights reserved.
doi:10.1016/j.jpowsour.2009.12.062

1. Introduction

Solid oxide fuel cells (SOFCs) are energy conversion devices that produce electricity by electrochemically combining a fuel and an oxidant across an ionic conducting oxide electrolyte. [1]

As it is regarded as the most efficient and versatile power generation system, SOFCs attracted more and more substantial interests in recent years [2,3]. Comparing to other kinds of fuel cell, the prominent advantage of SOFCs is fuel flexibility, offering the possibility for direct utilization of hydrocarbons and other renewable fuels [4]. This results in potentially higher overall fuel to electric efficiency of around 60% for single cycles and up to 85% efficiency for total systems [5].

General reaction mechanism of SOFC, except for the ones with proton conducting electrolyte, is shown in Fig. 1. The cell is composed of two porous electrodes and an ionic conductive ceramic electrolyte. At present, the most common materials for SOFCs are oxide ion conducting yttria-stabilized zirconia (YSZ) for the electrolyte, perovskites such as strontium-doped lanthanum manganese (LSM) for the cathode and nickel/YSZ for the anode. Oxygen gas is reduced to O^{2-} at the porous cathode and then is transported through the electrolyte to the anode. Finally, O^{2-} will react with H^+ to form water.

Modeling and simulation techniques have been used to improve understanding of the reaction mechanisms and kinetics of electrode processes in SOFCs. It has been well accepted that in intermediate-temperature SOFCs, oxygen reduction at the cathode is the main rate limiting factor to the performance of the whole system [6,7]. Numerous works on SOFC cathode modeling can be found in the literature. The porous structure and mixed conductivity property of SOFCs cathode make it difficult to obtain an exact model for the entire electrode process.

In this paper, the authors are trying to summarize the cathode modeling efforts in the last 20 years. Since the electrode reaction process description originated from the basic understanding of solid state physics and solid state electrochemistry, the properties of SOFCs cathode materials and related investigation methods will be introduced first. The oxygen reduction pathway is the fundamental part of the cathode model. Different conceptions on oxygen transport will be shown in the main part of this review. Furthermore, experimental methods which are utilized to verify SOFC cathode models also will be illustrated in this paper.

2. SOFC cathode materials

As mentioned above, oxygen reduction takes place at the SOFC cathode. The overall reaction can be written by Kröger–Vink notation as follows:

$$\frac{1}{2}O_2(g) + 2e' + V_{\ddot{O}} \rightarrow O_O^x \quad (1)$$

Materials which are used as the SOFC cathode must satisfy the conditions as below at high temperatures (between 500 and 1,000 °C, but more typically around 800 °C) [8]:

- Adequate electronic and ionic conductivity.
- High catalytic activity for oxygen reduction.
- Chemical stability and relatively low interactions with the electrolyte.
- High compatibility with other cell components.

During the early stage of SOFC development, platinum and some other noble metals were used as the cathode materials. However, platinum is expensive and its compatibility with the electrolyte is not so good. Recently, less expensive perovskites which also possess the required properties attracted much interest.

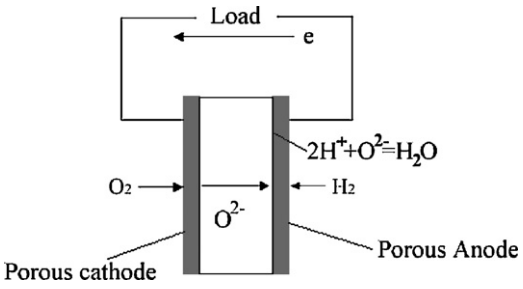

Fig. 1. Sketch of a single solid oxide fuel cell.

Fig. 2 reveals the lattice structure of ABO_3 perovskite. In general, in the perovskite-type structure, B site element is closely bonded to six oxygen atoms with a strong covalent nature, while A site element coordinates to 12 oxygen ions with a strong ionic nature. Most of the perovskites can be considered as cathode materials except perovskites which have a low electronic conductivity such as (La, Sr)(Mn, Fe)O_3, $YCoO_3$ or (Y, Ca)FeO_3 [9].

$La_{1-x}Sr_xMnO_{3\pm\delta}$ (LSM) is one of the widely used and researched cathode perovskite materials in SOFC. Those Sr-doped lanthanum perovskites show both large oxygen-excess under oxidizing atmosphere and large oxygen deficient when in reducing gas atmospheres [10]. Oxygen deficient is the result of the oxygen vacancies while oxygen-excess results on metal vacancies. It shows good electrode properties for YSZ electrolyte [11]. However, the oxygen ion conductivity of LSM materials and its oxygen trace diffusion coefficient is extremely low [12]. This poses practical limitations and restrictions to the application of LSM especially at low temperature (<800 °C).

Iron and cobalt-containing perovskite $La_{1-x}Sr_xCo_{1-y}Fe_yO_{3\pm\delta}$ (LSCF) is another candidate for SOFC cathode materials. Compared with LSM based materials, LSCF has higher ionic and electronic conductivity. Hence, some times LSM will be treated as an electronic conductor (EC) while LSCF is always referred as mixed ionic and electronic conductor (MIEC). [13] Although the use of LSCF as SOFC cathode can effectively enhance the cell's performance, LSCFs cathodes have to be selected carefully because they have a higher thermal expansion coefficient (TEC) than the YSZ electrolyte [14].

To lower the operating temperature of SOFCs, strontium-doped samarium cobaltite with composition of $Sm_{0.5}Sr_{0.5}CoO_3$ (SSC) has been studied recently. Its conductivity is much higher than LSCF and LSM at the low temperature (500–800 °C) [15,16]. On the other hand, just as for LSCF, the TEC of SSC is too large and it will affect its compatibility with the YSZ electrolyte. However, it is particularly compatible with GDC and LSGM. [17].

As illustrated above, the TEC of LSM is close to YSZ but its ionic conductivity is very low. The electronic and ionic conductivities of LSCF and SSC are high but their TEC are much higher than YSZ. Therefore, many alternative materials have been studied with the aim of increasing ionic conductivity and obtaining a TEC close

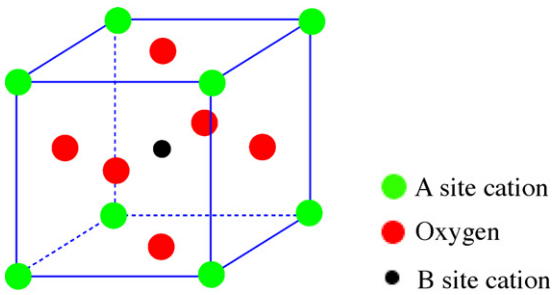

Fig. 2. Schematic representation of lattice structure of perovskite, ABO_3.

to the TEC of YSZ. For example, Fe-substituted lanthanum strontium cuprate ($La_{0.7}Sr_{0.3}Cu_{0.4}Fe_{0.6}O_{3-\delta}$) was reported to present a high conductivity and good thermal expansion match to SDC [18]. $Ba_{0.5}Sr_{0.5}Co_{0.8}Fe_{0.2}O_{3-\delta}$ (BSCF) is another attracted cathode material for intermediate-temperature SOFCs [19].

2.1. Conductivity

Perovskite structure oxides receive much attention on their conductivity properties since they are widely used as SOFC cathodes. According to the classification of solid state electrochemistry, SOFC cathodes belong to intercalation electrodes category. The existence of host particles and guest particles results in the conductivity. The host particles provide a lattice or framework; the guest particles occupy sites within this framework. There are two special properties for intercalation compounds: the guests are mobile, moving between sites in the host lattice; and the guests can be added to the host or removed from it, so the concentration of guests can change [20].

2.1.1. Electronic conductivity

Generally, it was thought that B site metal vacancy was the electronic carrier for perovskite structure mixed conductor. For $La_{1-x}Sr_xMnO_{3\pm\delta}$, manganese usually was considered as having three oxidation states Mn_B^x (Mn^{3+}), Mn_B' (Mn^{4+}) and Mn_B'' (Mn^{2+}).

In Finn Willy Poulsen's work [21], the electrical conductivity of LSM was considered in the range from 1 to 250 S cm^{-1} going from room temperature to 1000 °C. The conductivity increases with the amount of Sr-doping up to $x = 0.5$. Poulsen explained the electrical conductivity of LSM by charge-transfer reactions between the different oxidation state manganese. He claimed electrons might transfer from a manganese ion, in one oxidation state, to neighboring manganese in a higher/lower oxidation state, possibly via an oxygen ion:

$$Mn_B' + Mn_B^x \overset{O_O^x}{\Leftrightarrow} Mn_B^x + Mn_B' \quad (2)$$

$$Mn_B' + Mn_B^x \overset{O_O^x}{\Leftrightarrow} Mn_B^x + Mn_B' \quad (3)$$

Mizusaki utilized a multi-level hopping model [22] to analyze the electrical conductivity of LSM [23]. He thought the electrical conductivity of LSM was essentially determined by the electronic state of d electrons of Mn. In his model, Mn_B' was considered accept electrons from Mn_B^x and Mn_B''. Besides, Mizusaki studied the conductivity as a function of mean Mn valence which was calculated from electrical neutrality of assuming the valence in other ions fixed to La^{3+}, Sr^{2+} and O^{2-}. It was concluded that electrical conductivity of oxygen-deficient composition LSM was essentially determined by the mean Mn valence, whether determined by the Sr doping or the non-stoichiometric deviation.

2.1.2. Ionic conductivity

Ionic conductivity of the perovskite-type oxides is caused by oxygen ion transportation. Mizusaki did some research on the relationship between the oxygen ions and the defects in the perovskite-type oxides [10,24]. Numerical relationships had been found in both of oxygen-deficient and oxygen-excess regions. Maximum and minimum values of the oxygen stoichiometry had been calculated based on the defect equilibrium.

Compared to electrical conductivity, ionic conductivity of LSM is much smaller. Therefore, it is difficult to measure the ionic conductivity of LSM from experiments without electrical conductivity affects. Huang [25] and his coworkers tried to measure the ionic conductivity of LSM. They used YSZ layer to block the electronic flows in the experiment. According to Huang's research, the ionic conductivity of LSM will vary in the range of $10^{-7.3}$ to 10^{-6} S cm^{-1} when the oxygen partial pressure is in 10^{-3} to 1 atm. Further, Endo et al. [26] have determined the oxygen ion conductivity in LSM in the pressure range 10^{-1}–10^{-3} atm oxygen at 800 °C to be 5.9×10^{-8} S cm^{-1} by the Hebb–Wagner technique.

There are two major steps involved in oxygen transportation—surface adsorption and bulk diffusion. Accordingly, two parameters, oxygen surface exchange coefficient (k) and oxygen diffusion coefficient (D), are applied to characterize the oxygen flux. These two parameters are very important for the investigation of SOFCs cathode reaction kinetics.

Typically, two kinds of experimental methods can be used to obtain D and k. One of them is known as isotope exchange depth profile (IEDP) [27] method. Isotope O^{18} is used in the experiment and the diffusion profile within the sample was determined by secondary ion mass spectrometry [28]. The other experimental method is named electrical conductivity relaxation (ECR). An abrupt oxygen partial pressure change is applied and the total conductivity will be measured until the sample reaches a new equilibrium state [29].

IEDP and ECR are both set up based on Fick's second law and both require dense samples since porosity influence is not considered in the data treatment processes. For IEDP method, the sample usually will be first annealed in the labeled $^{16}O_2$ atmosphere for a long time, which is approximately one order of magnitude greater than the tracer anneal time, to make sure the sample is in chemical equilibrium in the desired temperature and atmosphere. Then the sample will be quenched to room temperature and reheated with the $^{18}O_2$ gas. Then ^{18}O penetration profile will be determined by SIMS. During this process, the rate of isotope exchange across gas/solid interface is assumed to be directly proportional to the difference in isotope concentration between the gas and the solid. This leads to the boundary condition:

$$-D\frac{\partial C}{\partial x} \mid = k(C_s - C_g) \quad (4)$$

C_g and C_s refer to the ^{18}O fraction in the gas phase and at the sample surface respectively [30–34].

For ECR method, the sample's total conductivity is assumed related with the oxygen stoichiometry. With a small oxygen partial pressure step change (usually $\Delta \log P_{O_2} \leq 1$), the relationship between the conductivity and stoichiometry, as shown below, is reasonable

$$\frac{\sigma(t) - \sigma(0)}{\sigma(\infty) - \sigma(0)} = \frac{d(t) - d(0)}{d(\infty) - d(0)} \quad (5)$$

$\sigma(t)$, $\sigma(0)$ and $\sigma(\infty)$ represent for the real time conductivity value, initial conductivity value and the equilibrium conductivity value, respectively. In addition, $d(t)$, $d(0)$ and $d(\infty)$ represent for the d value of ABO_{3-d} respectively for the real time, initial point and the equilibrium point [35].

Therefore the measured conductivity values can be used for solve the diffusion equation. Corresponding boundary condition is:

$$-D\frac{\partial C}{\partial x} \mid = k(C_\infty - C_S) \quad (6)$$

C_∞ is the equilibrium surface oxygen concentration and C_s is the real time surface concentration [36].

For both of IEDP and ECR methods, the diffusion equation's solutions are different according to the sample's shape [37]. Pellet samples are generally used since the diffusion process can be simplified to a 1D model. At the same time, cylinder shape samples also had been studied by some researchers [10].

Compared to using isotope, ECR testing method is much easier to carry out and offers significant cost-advantage. Much work has been done on ECR testing recently [38–41]. However, this measuring method can only be applied for uniform, single-sample, while

composite, porous cathodes have been used for SOFCs to get high performance. Therefore, it is necessary to improve the ECR or IEDP method to make the parameters obtained is more meaningful for the cathode process study.

2.2. Electro-catalytic property for oxygen reduction

The oxygen reduction catalytic property of perovskite-type oxides is related closely to their ionic conductivity. Electro-catalytic property improvement will result in oxygen surface exchange rate increase. It can extend the active reaction area from TPB (three-phase boundary where gas, electrode and electrolyte meet) to gas/electrode interface. And the active area extension will improve the fuel cell performance.

Bell [42] investigated influence of different synthesis routes on LSM catalytic properties. Six different synthesis ways including solid state reaction, drip pyrolysis, citrate, sol–gel, carbonate and oxalate co-precipitation had been utilized in this study. Temperature-programmed reduction (TPR) and temperature-programmed reaction (TPRxn) experiments which were performed in CO_2 or CO, O_2 mixed gas were applied to test the catalytic properties of LSM. Based on their analysis results, LSM made by the citrate method was the most suited to oxidation catalysis. Mars van Krevelen and ionic redox models were used to explain the oxygen reduction mechanism at low temperature and high temperature (>550 °C) separately. And Robert claimed that the oxygen reduction at low temperature was associated with the intrinsic oxygen vacancies while the reaction at high temperature was due to the manganese reduction from Mn^{4+} to Mn^{3+}.

Kan and co workers used the temperature-programmed isotopic exchange method to investigate the catalytic property of modified LSM and LSCF [43,44]. They claimed that for ABO_3 the A site elements did not produce significant change in isotopic exchange. Cobalt infiltration improved the performance of LSM the most while iron reduced the apparent activity.

On the contrary to the above mentioned research, Kammer indicated that the A site elements will affect the electro-catalytic properties of the perovskite [45]. He investigated Fe–Co based perovskite with different A site elements. According to the experimental results, Kammer thought perovskite with small A site elements possesses high electro-catalytic properties. He offered two possible explanations in his work. One is that when the size of the A site cation is lowered a small amount of a cubic perovskite phase emerges. The cubic phase might have a high activity for oxygen reduction. Another one is with small A site cations, two-perovskite-phase system is formed. This unique microstructure might enhance the catalytic property for oxygen reduction.

Besides improving the cathode material itself, making composite material is another way to improve cathode electrochemical properties. Serra and Hans-Peter [46] added Pd into the cathode material to improve its electro-catalytic property. The improved materials were prepared by contacting the LSM and LSCF powder with Pd and Rh nitrates aqueous solution under stirring at 80 °C for 5 h. Li et al. [47] developed three different NiO-based composite cathode catalysts for electrochemical oxidation of hydrogen sulfide in intermediate-temperature solid oxide fuel cells.

2.3. Summary

Basic chemical and physical properties of perovskite materials had been shown in this part. Because the perovskite-type oxides possess mixed electronic and ionic conductivity, the oxygen reduction region will be extended. The mixed conductivity of perovskite was thought associated with the valence change of B site element and the oxygen vacancies which is caused by the doped elements. Furthermore, the oxygen mass transport was generally divided into surface exchange and bulk diffusion, two continuous processes. Kinetic parameters can be measured by isotope exchange or electrical conductivity relaxation methods. Although basic understandings on the perovskite materials had been developed, the knowledge we have now are still not sufficient enough to offer a full picture. And due to the limitation of the experimental methods, the kinetic parameters obtained were just approximation values. The lack of knowledge of cathode materials intrinsic properties made the modeling work of SOFCs cathode electrode more difficult.

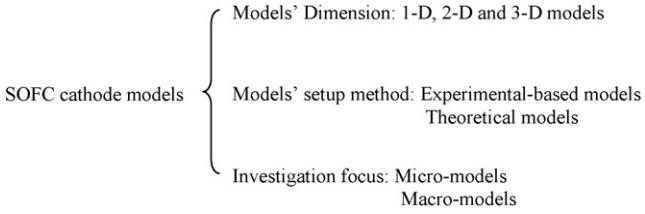

Fig. 3. Different classifications of SOFCs cathode models.

3. SOFC cathode models

The electrode reaction mechanism is a fundamental issue for electrochemistry study. A reliable elucidation includes useful information on how to improve cell performance. Limited by the development of solid state ionic conductivity theories, researchers began to try to build up SOFC cathode models over the past 20 years.

Aqueous solutions are the traditional electrochemical system. Therefore, generally accepted conclusions and common investigation methods of aqueous system are the basis for SOFC cathode studies. However, the solid state system is more complex compared with the aqueous system. First, three-phase boundary (TPB), where gas molecular, cathode and electrolyte materials meet, exists stably in SOFCs. At the same time, at the cathode side gas/cathode and cathode/electrolyte two-phase boundaries (2PB) also exist. It brings several possible pathways for oxygen reduction. Second, in aqueous systems only ion diffusion occurred while for SOFC cathodes oxygen gas and ions will diffuse against the electrons. Finally, the double layer formed on the electrode is different. For aqueous system, usually the inactive ions in the solution will move to the electrode surface under the electrical field. However, on the surface of SOFC cathode, adsorbed atomic oxygen or ions will form the double layer.

SOFCs cathode models can be classified by different levels. As shown in Fig. 3, according to the dimension of the model, there are 1D, 2D and 3D models. Further, according to the model's setup method, some literature modeled SOFC cathodes in the viewpoint of theory while others utilized experimental data to set up their models. For example, some studies about three-phase boundary had been done based on the SEM morphology results. Finally, according to different investigations, SOFC cathode models can be divided to micro-models and macro-models. The former studies the detailed cathode reaction steps and the latter one mainly considered the entire effect of the factors such as porosity, gas flow rate, temperature, etc. In this review, we will follow the third way to give an introduction of the SOFC cathode modeling development.

3.1. Micro-models

Researchers always focus on the detailed oxygen reduction steps and the electrochemical affects. The geometry factors will be ignored or simplified as a parameter. Thus far, the most arguable issue is whether the reduction reaction is controlled by a chemical process or an electrochemical process. In this part, representative

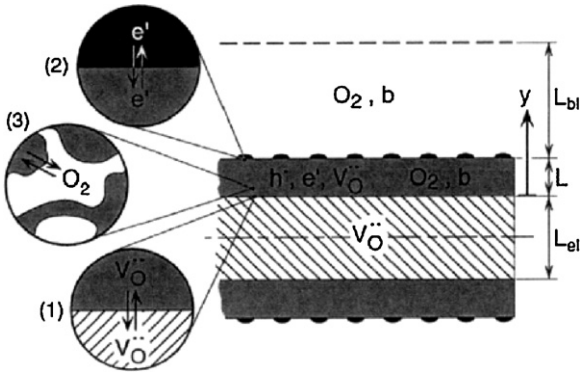

Fig. 4. Cell geometry in Adler's model [48].

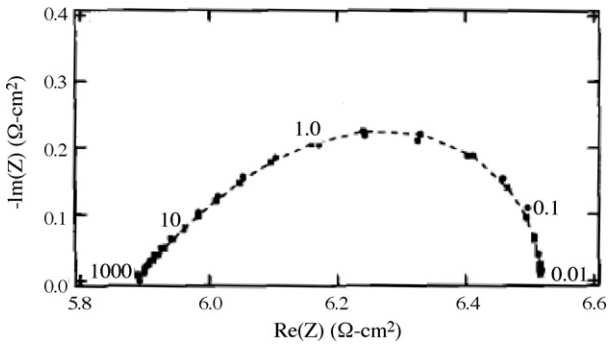

Fig. 5. Plot of measured (circles) and calculated(squares) complex impedance of a symmetrical cell in air at 700 °C [48].

works based on these two different understandings will be introduced.

3.1.1. Pure chemical process

Adler is one of the early researchers who treated the SOFCs cathode reaction as a pure chemical process. In the model developed in 1996, as shown in Fig. 4, Adler et al. [48] specified the overall cathode reaction occurred via three separated interfacial reactions: (1) charge-transfer of oxygen ion vacancies across the cathode material/electrolyte interface; (2) charge-transfer of electrons across the current collector/cathode material interface; (3) chemical exchange of oxygen at the gas/cathode material interface. Due to the last specification, this model can only be valid for the mixed conductors with high rates of oxygen surface exchange, such as LSC.

The contributions to cathode kinetics were claimed as only the diffusion of oxygen and exchange of O_2 at the mixed conductor/gas interface. To illustrate the chemical contribution, either one of the non-charge-transfer steps would be considered as the rate limited step of the entire cathode reaction. Their models showed, when the surface exchange and solid state diffusion dominated, the total cell impedance would reduce to:

$$Z = R_{\text{chem}}\sqrt{\frac{1}{1+j\omega t_{\text{chem}}}} \tag{7}$$

When the gas phase diffusion was the limit, the total cell impedance was:

$$Z = \frac{R_{\text{gas}}}{1-j\omega R_{\text{gas}}C_{\text{gas}}} \tag{8}$$

R_{chem} and R_{gas} are characteristic resistance, t_{chem} is a time constant and C_{gas} is the effective capacitance with gas phase diffusion polarization. Their results showed that the bulk properties of the cathode material would quantitatively affect the electrode kinetics. In order to verify this simulated result, Adler et al. compared the measured ac response of a symmetrical cell, which was composed of two $La_{0.6}Ca_{0.4}Fe_{0.8}Co_{0.2}O_{3-\delta}$ electrodes and $Ce_{0.9}Sm_{0.1}O_{2-x}$ electrolyte, with the predicted results. As Fig. 5 presents, the measured plots agreed well with the calculated results.

Additionally, in this model work, Adler brought out the concept of a characteristic distance which indicated the extension of the reaction zone beyond the three-phase boundary. The chemical resistances corresponding to different characteristic distances were calculated based on the model. The best extension distance was expected to be few microns.

As in the early mixed conductor cathode modeling, Adler's work offered lots of valuable understanding for the reaction mechanism. However, there also existed many arguable parts [49]. People doubted whether it's reasonable to define all the reduction reactions occurring at the electrode/gas interface. Besides, if the oxygen would be reduced, why is the oxygen surface exchange defined as a non-charge-transfer reaction. Adler explained their idea in a following paper [50], and he believed the oxygen reduction should only happen on the electrode/gas interface since matter cannot pass through a truly three-phase boundary. Furthermore, the processes of "charge-transfer" and "non-charge-transfer" had been defined. "Charge-transfer" represented any step that involves charged species and driven directly by gradients in electrical state and always occurs at a rate proportional to the current. On the other hand, "non-charge-transfer" process is any step that involves neutral species or neutral combinations of species. It is driven by gradients in chemical potential and occurs at a rate independent of current.

Symmetrical cells under three different conditions were discussed in this paper. Finally, the author concluded that the oxygen reduction was limited by the oxygen diffusion. And the diffusion process was independent with the electrochemical factors since oxygen molecular was neutral particles. It should be pointed that this model ignored the effects of electron and oxygen vacancy concentrations inside the mixed conductor. As the main participants, they would certainly affect the oxygen reduction reaction. Furthermore, since those particles are chargeable, electrochemical conditions may control their diffusion process. Therefore, Adler's model may be more suitable for the period when the fuel cell starts running.

Svensson et al. [51,52] developed a physical model to show the possible oxygen transport pathways on SOFC cathodes. As shown in Fig. 6, the first step of oxygen reduction is adsorption

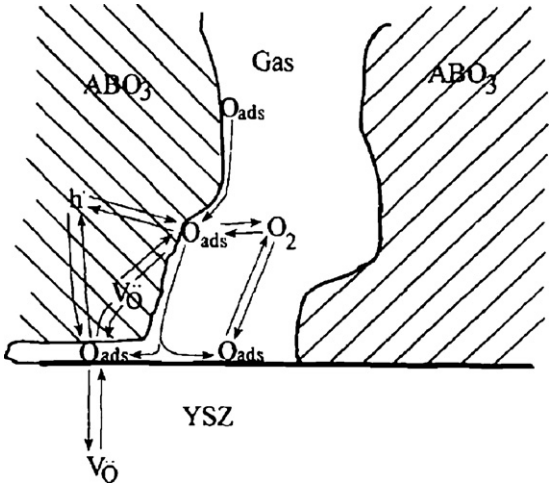

Fig. 6. Sketch of Svensson's two step reactions cathode model [52].

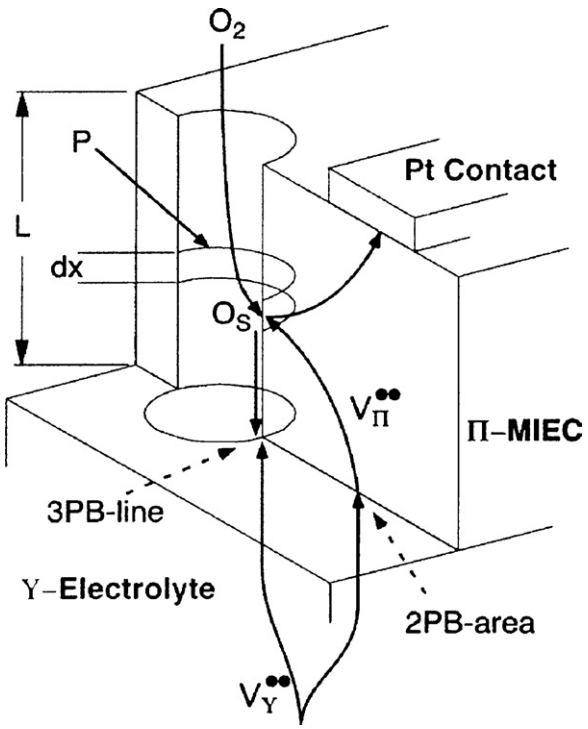

Fig. 7. Cross-sectional schematic of the physical structure and chemical reactions occurring at porous SOFCs cathode [53].

and desorption of neutral, monatomic oxygen at the gas/cathode and gas/electrolyte interfaces. Then the absorbed oxygen atom will combine with the vacancy to form oxygen ion. The two step reactions can be written as:

$$O_2(g) + 2ads \underset{k_{des}}{\overset{k_{ads}}{\rightleftarrows}} 2O_{ads} \tag{9}$$

$$O_{ads} + V_O^{\bullet\bullet} \underset{k_o}{\overset{k_r}{\rightleftarrows}} ads + 2h' + O_o^x \tag{10}$$

Svensson postulated that the interface between cathode and electrolyte contained intermediate oxygen species. Those species would either combine with the vacancies of the cathode material or combine with the vacancies of the electrolyte material. The reaction occurring at the gas/cathode interface was considered chemical in nature since no interfacial charge-transfer was involved, while the one occurring at the electrolyte surface was considered as an electrochemical process. Therefore, different from Adler's model, Svensson et al. introduced overpotential into their simulation to express the departure of the surface exchange reaction occurring at electrolyte surface from equilibrium. According to Svensson's numerical results, a limiting current was predicted at high overpotential due to depletion of oxygen at the cathode/electrolyte interface, and they found there was a correlation between the limiting current and $P_{O_2}(i \propto P_{O_2}^n)$. When the exchange process was the limited rate step for the cathode reaction, the value of n was between 0.58 and 0.74. Smaller n values ($0.26 < n < 0.56$) was predicted for a slow adsorption process. However, the two oxygen pathways in Svesson's model were considered in separate simulations.

By the approach of Svesson, the influence of surface and bulk transport pathways for SOFC cathode can be described, but it is not possible to quantitatively compare the contribution to the total current by each path. To solve this problem, Coffey et al. [53] presented a continuum model which simultaneously considered both pathways, as illustrated in Fig. 7. They considered oxygen may transport through the triple-phase boundary (3PB) between the electrolyte, gas and cathode or the two-phase boundary (2PB) between the cathode and electrolyte. B-V equations for the surface overpotentials were taken as the boundary conditions in this model's simulation. Since that the total voltage drop across the cathode–electrolyte interface is independent of the transport path chosen, by setting one surface overpotential the overpotential for the other path can be calculated. However, although Coffey treated the reactions occurring at 3PB and 2PB interfaces as electrochemical motivated reactions, oxygen reduction occurring at gas/cathode interface was considered as chemical reaction due to the fact that no net charge was gained or lost by the cathode.

In 2006, researchers from NASA set up a SOFC model for system controls and stability design [54]. The cathode reaction process was considered associated with oxygen absorption, desorption, diffusion and electronation. The charge-transfer pathways can be presented as below:

$$O_2(g) + 2s \overset{k_{ad},k_{des}}{\longleftrightarrow} 2O_{ad} \tag{11}$$

$$O_{ad} + V_{\ddot{O}} + 2e^- \overset{k_{lc},k_{-lc}}{\longleftrightarrow} O_O^x + s \tag{12}$$

where s is the concentration of vacant surface sites.

As we can see from the cathode mechanisms stated above, researchers considered the oxygen reduction as a pure chemical reaction because they thought there was no net charge-transfer chargeable intermediate at the interface. However, during the real oxygen reduction process chargeable intermediates are possibly formed. Furthermore, although there may be no net charge transfer at the reaction interface, some researchers hold the point that the reaction should be considered as an electrochemical process since its reactants and products are chargeable particles.

3.1.2. Electrochemical process

Considering oxygen reduction is a reaction involving chargeable particles, most researchers hold the point that the cathode reaction of SOFC was an electrochemical process. It is well-accepted that the surface overpotential should be an important factor to the entire cathode reaction process. Besides, the researchers also claimed oxygen reduction can not be finished in one step which means there will be some intermediates during the reaction process. And the absorbed chargeable intermediates also will be affected by the surface overpotential.

Liu and Winnick investigated the reactions occurring on MIEC/gas interface. They considered oxygen reduction involving several intermediates as shown in Fig. 8 [55]. Possible reaction pathways are shown below.

Further, Liu et al. discussed the electrical state effects on the rate of interfacial reactions. Based on their analysis, the oxygen reduction rate depended critically on the electrical states of the MIEC/gas surface. Hence the reaction was confirmed as electrochemical reactions.

van Heuveln [56] considered O^-, O_2^- existed during the oxygen reduction process. And he assumed there were three possible charge-transfer pathways. $La_{0.85}Sr_{0.15}MnO_3$ cathode was prepared by tape casting on a presintered YSZ pellet. Electrochemical resistance and Tafel plots were measured to verify van Heuveln's model. The experimental results indicated that diffusion of O_{ad}^- species along the LSM surface to TPB area will compete with charge-transfer at low overpotential. The diffusion limitation disappears at high cathodic overpotentials. On the other side, the model's simulation results also show that the diffusion process is influenced mainly by the current. However, in van Heuveln's model, the reduction occurring at the gas/cathode interface was ignored. MIEC was

treated similar to the metal electrode.

$$\text{Model 1}\quad \begin{aligned} &O_2(g) \rightarrow 2O_{ad}\\ &O_{ad} + e \rightarrow O^-_{ad}\\ &O^-_{ad} \rightarrow O^-_{TPB}\\ &O^-_{TPB} + e + V^{\cdot\cdot}_O \rightarrow O^x_o \end{aligned} \tag{13}$$

$$\text{Model 2}\quad \begin{aligned} &O_2(g) + e \rightarrow O^-_{2,ad}\\ &O^-_{2,ad} + e \rightarrow 2O^-_{ad}\\ &O^-_{ad} \rightarrow O^-_{TPB}\\ &O^-_{TPB} + e + V^{\cdot\cdot}_O \rightarrow O^x_o \end{aligned} \tag{14}$$

$$\text{Model 3}\quad \begin{aligned} &O_2(g) + e \rightarrow O^-_{2,ad}\\ &O^-_{2,ad} \rightarrow O^-_{2,TPB}\\ &O^-_{2,TPB} + e + V^{\cdot\cdot}_O \rightarrow O^x_O + O_{ad}\\ &O_{ad} + e \rightarrow O^-_{ad}\\ &O^-_{ad} + e + V^{\cdot\cdot}_O \rightarrow O^x_O \end{aligned} \tag{15}$$

Mitterdorfer [57] also thought O^-, O^-_2 may exist during the reduction process. He developed a physical model to explain oxygen transport from the LSM cathode to the YSZ electrolyte. The reactions can be described as follow:

$$O_2(g) + e^- + s \Leftrightarrow O^-_2(ad) \tag{16}$$

$$O^-_2(ad) + e^- \Leftrightarrow 2O^-(ad) \tag{17}$$

$$O^-(ad) + e^- + V^{\cdot\cdot}_O \Leftrightarrow O^x_O + ad \tag{18}$$

In Mitterdorfer's model, LSM had been considered as pure electronic conductivity. The oxygen ions were assumed only can be formed at TPB area.

Chan et al. [58] developed a micro-model for an LSM electrode. All possible polarizations which govern the complex interdependency among the transport phenomena, electrochemical reaction and microstructure of the electrode and their combined effect on the cathode overpotential under different operating conditions had been considered in this model. They claimed that when the applied oxygen partial pressure was lower than 0.1 atm, a third arc can be seen in the low frequency band of impedance spectra which is due to gas phase diffusion.

Chan applied the reaction steps of van Heuveln's model 1 to develop their model. The difference is that Chan et al. established a correlation between the microstructure and the performance of the cathode. According to the simulation results, it was found that the larger the particle size is the thicker the cathode should be for reduced cathode overpotential. Furthermore, the current density and oxygen partial pressure were found not to effect on the optimal electrode thickness value. However, it will affect on the optimal particle size.

Bilge Yildiz presented a two-dimensional physical model that takes into account the effect of both surface and bulk pathways under different operating conditions and electrode configurations [59]. The possible surface and bulk pathways were shown below, and AC impedance spectra of LSM electrode were applied to verify Bilge's model:

$$\text{Model 1}\quad \begin{aligned} &O_2 \Leftrightarrow 2O_{ad,s}\\ &O_{ad,s} + e^- \Leftrightarrow O^-_s\\ &O^-_s \Leftrightarrow O^-_{3PB}\\ &O^-_{3PB} + e^- \Leftrightarrow O^{2-}_{3PB}\\ &O^{2-}_{3PB} + V^{\cdot\cdot}_{\underset{O}{}} \Leftrightarrow O^Y_O \end{aligned} \tag{19}$$

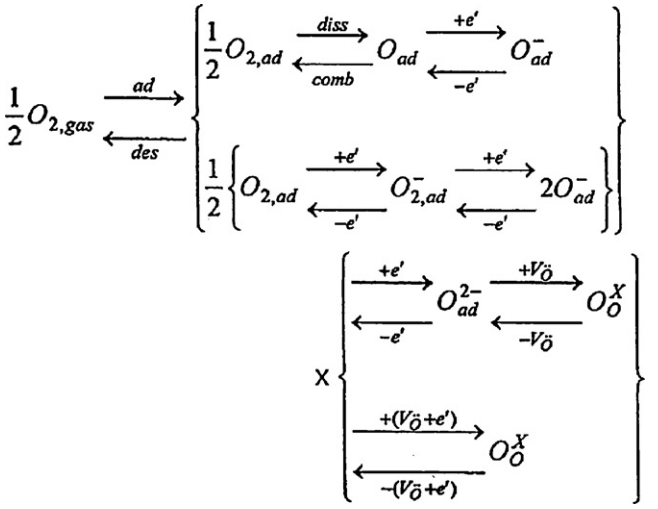

Fig. 8. Possible oxygen reduction process by Liu et al. [55].

$$\text{Model 2}\quad \begin{aligned} &O_2(g) \Leftrightarrow 2O_{ad,s}\\ &O_{ad,s} \Leftrightarrow O_{3PB}\\ &O_{3PB} + e^- \Leftrightarrow O^-_{3PB}\\ &O^-_{3PB} + e^- \Leftrightarrow O^{2-}_{3PB}\\ &O^{2-}_{3PB} + V^{\cdot\cdot}_{\underset{O}{}} \Leftrightarrow O^Y_O \end{aligned} \tag{20}$$

To prove that the intermediates are likely to exist during the oxygen reduction process, Liu et al. investigated the oxygen reduction process on a silver electrode surface using the first-principles calculations based on the density functional theory and pseudopotential method [60]. The calculation results suggest that the oxygen reaction on silver cathode can be described like this:

$$O_2(g)(+e) \rightarrow O^-_2(+e) \rightarrow O^{2-}_2(+2e) \rightarrow 2O^{2-} \tag{21}$$

Since in this work a metal electrode has been studied, the calculation results show that the oxygen reduction and the incorporation of the dissociated O ions in the oxide electrolyte prefer taking place in the TPB region. For MIEC electrodes, due to the fact that oxygen vacancy may exist inside the material, the reduction process will not only occur near TPB region. However, although this work offers some evidence for the intermediates, it's not so convincing that they will appear in perovskite MIEC. Therefore researchers still worked on finding some new ways to verify the existence of the intermediates and to confirm what kind of intermediates will appear during the reduction process.

Since researchers considered the cathode reaction as an electrochemical process, surface overpotential needs to be introduced into their simulations. To make a clear idea on this issue, first we need to know what the overpotential is and how it is generated. Overpotential refers the potential difference between a half-reaction's thermodynamically determined reduction potential and the potential at which the redox event is experimentally observed. For an aqueous system, the overpotential is formed at the electrode/electrolyte interface. For the SOFC cathode, the overpotential exists not only at the electrode/electrolyte interface but also at the gas/electrode interface and the TPB area. And there are three different parts for the overpotential: overpotential caused by the material's resistance, overpotential caused by the surface exchange process and overpotential caused by the oxygen ion diffusion.

Fleig [61] discussed MIEC surface overpotential which is caused by surface charge transfer. Fig. 9 is given to show the overpotential difference between a liquid electrolyte system and SOFCs cathode.

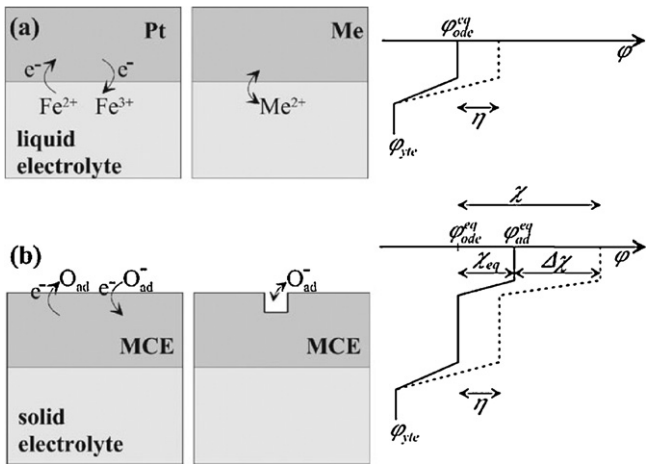

Fig. 9. Sketches of electron and ion transfer reactions at (a) metal/liquid electrolyte and (b) mixed conducting electrode (MCE)/solid electrolyte interfaces [61].

For a metal electrode in aqueous electrochemical system, electron and ion transfer only occurred at the electrode/electrolyte interface so the overpotential can only be formed at the electrode/electrolyte interface. However for mixed conducting electrode, electron and ion transfer also occurred at the electrode/gas interface. Hence it is necessary to introduce the item of surface overpotential change $\Delta\chi$ into the simulation. Fleig discussed the application of $\Delta\chi$ under electron transfer step control and ion transfer step control conditions. He also studied the relationship of MCE surface overpotential ($\Delta\chi$) and electrode/electrolyte interface overpotential (η).

In their later work, the equivalent circuit based on the understanding of the oxygen reduction pathways was presented, as Fig. 10 shows [62,63]. $La_{0.6}Sr_{0.4}Co_{0.8}Fe_{0.2}O_{3-\delta}$, $Ba_{0.5}Sr_{0.5}Co_{0.8}Fe_{0.2}O_{3-\delta}$ and $Sm_{0.5}Sr_{0.5}CoO_{3-\delta}$ thin films were applied to study the oxygen reduction. Thin films and patterned electrodes are usually used for investigating the overpotential effects because it is possible to precisely control the geometry related to the triple phase boundary and bulk reaction pathways. Based on the ac and dc resistance measurements, Fleig claimed that the capacitance in Fig. 10 was a constant phase element ($Q^{-1}(i\omega)^{-n}$) and the exponents close to one. And they found for the investigated materials, the oxygen exchange reaction on the MIEC surface limited the kinetics of the overall oxygen reduction reaction. On the other hand, according to the experimental results, $Ba_{0.5}Sr_{0.5}Co_{0.8}Fe_{0.2}O_{3-\delta}$ exhibited the lowest surface-related polarization resistance compared to the other two materials.

Liu developed a 2D model based on Fleig's theory of MIEC surface overpotential [64]. Fig. 11 depicts their model geometry. As Fig. 11b shown, the dashed-line box in Fig. 11b is the two-dimensional investigated region.

The gas exposure surface reactions were assumed as below:

$$\frac{1}{2}O_2 + s \rightarrow O'_{ads} + h' \quad (22)$$

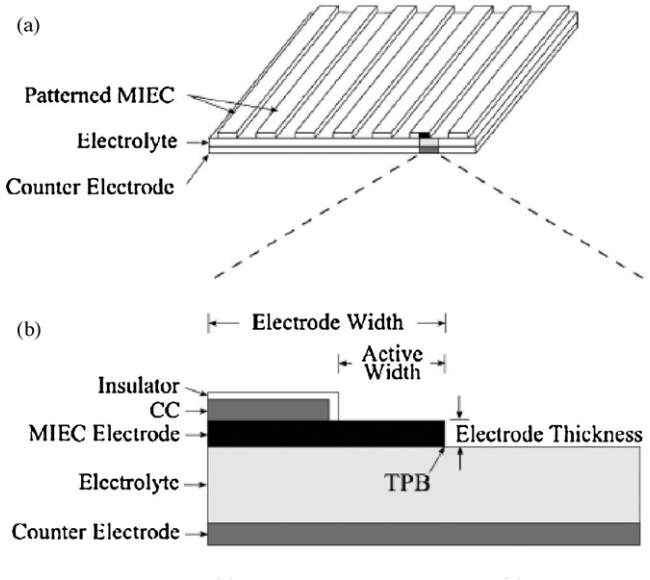

Fig. 11. Sketch of 2D model [64].
(a) Patterned electrode array and (b) Symmetric 2D cross-sectional model domain.

$$O'_{ads} + V_O^{\cdot\cdot} \rightarrow O_o^x + h' + s \quad (23)$$

The reaction rate had been discussed in their previous work [65]. The simulation results show that under low overpotential the ionic transportation will be the rate limiting step which means low overpotential (50 mV) does not affect predominately on oxygen reduction. Under high overpotential (750 mV), the sheet resistance will be the main factor of the reaction rate which means that the surface exchange step will be the rate limiting step.

3.2. Macro-models

Macro-models are set up based on the oxygen reduction mechanisms offered by the micro-models as introduced above. Compared to micro-models, macro-models pay more attention on the effect of the physical factors such as the electrode porosity, gas flow rate, temperature and so on.

Janardhanan [66] presented a mathematical model to calculate the volume specific three-phase boundary length in the porous composite electrodes of SOFC. They assumed all the ionic and electronic conductive particles were spherical particles. The influence of grain size and porosity on the volume specific TPB length had been investigated separately for the uniform and non-uniform particle size distribution.

Composite cathodes attracted more attention recently since they exhibit much lower overpotential than single-phase electrodes by the virtue of parallel paths for ionic and electronic charge carriers. Moreover, the use of a composite cathode allows a spreading of the reaction zone from the electrode/electrolyte interface

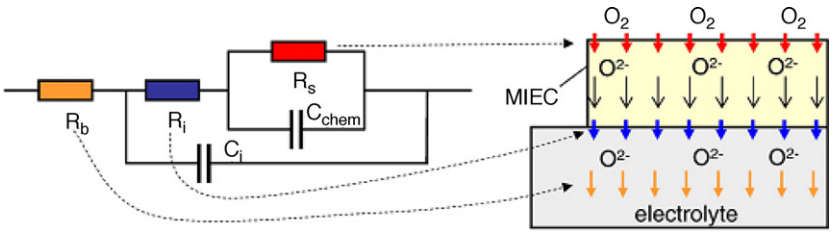

Fig. 10. An equivalent circuit of the MIEC electrode and the sketch of the oxygen reduction process [62].

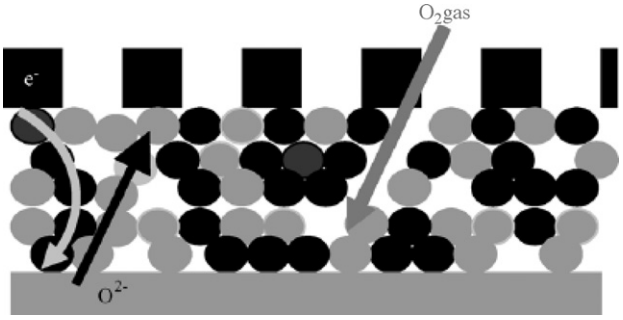

Fig. 12. Schematic representation of a monodisperse porous YSZ–LSM cathode. Black circles: LSM grains; grey circles: YSZ grains; empty space: gas filled pores. [68].

into the electrode. To obtain better optimization composite cathodes, some theoretical investigations have been done.

Ali Abbaspour et al. [67] developed a new rigorous model to study the structure performance relationship of SOFC cathodes. Their work consisted of the following steps: First, creating a random matrix of electronic and ionic conductor particles; second, transforming the data to a geometrical form; and last, model the transport and reaction process in each domain using a multi-physics solver. Their simulation results showed that the electrode-electrolyte interface is not always the high reaction rates region. This can happen when the porosity of electrode is not enough to transport the oxygen to reaction sites. Moreover, they discussed the relationship between the polarization resistance and LSM volume fraction of the LSM/YSZ composite electrode.

Deseure et al. [68] utilized a chemical model to optimize the percolation rate of LSM + YSZ composite electrode. They considered LSM as a pure electronic conductor and therefore the oxygen reduction was assumed to occur at a three-phase boundary, as Fig. 12 shows. And in their model the effective ionic conductivity can be calculated by the following equation:

$$\kappa^{\text{eff}} = T_{\text{per}}\varepsilon_a \frac{1-\varepsilon}{\tau}\kappa \tag{24}$$

where T_{per} is the percolation rate (ionic + electronic); κ the ionic conductivity of YSZ; ε_a the volume fraction of YSZ; ε the porosity and τ the tortuosity. Besides, the relationship between percolation rate and YSZ volume fraction had been studied. As a result, the author thought a graded composite electrode was the best way to increase the oxygen reduction rate.

Deseure et al. [69] presented a chemical model to investigate the effect of electrode thickness, grain diameter and pore's diameter for a LSM/YSZ composite electrode. The microstructure parameters will affect surface adsorption area and the ionic conductivity of MIEC. They claimed that when the volume fraction of YSZ was 0.5, decreasing the grain diameter improves electrode performances.

Since the cathode electrode is a complex system, computational methods were used widely for simulation. Monte Carlo methods are a class of computational algorithms that rely on repeated random sampling to compute their results. The methods are useful in studying systems with a large number of coupled degrees of freedom and for modeling phenomena with significant uncertainty in inputs. Yan Ji et al. used this method to develop a 3D micro-scale model to simulate the transport and electrochemical reaction in a composite cathode [70]. They split the entire composite cathode into two sub-networks: an electrical network for the solid phase and a pore network for the void space. The species concentrations and chemical reaction rate will be calculated within the pore network, whereas the charge transfer, resistances and overpotentials will be analyzed within the electrical networks. Their results demonstrated that the electrochemical reaction behavior was strongly influenced by the porosity value. And small particle sized will reduce activation overpotential by increasing the TPB length per unit volume of the cathode but at the same time too small particle will increase the gas diffusion resistance.

Martinez and Brouwer also developed a Monte Carlo model to characterize the factors controlling triple phase boundary formation in SOFC cathode [71]. Their model accounted for electronic conductor, ionic conductor and gas phase percolation. Competition between percolation of gas and electronically conducting phases had been considered in this model. Fig. 13 demonstrated a sample of randomized monodispersed interface structure that is utilized in Martinez's model. Two major portions of the model are composed of the formation of a randomized composite electrode structure and the analysis of the randomized structure. To obtain statistical significance, 10,000 random interface instances were analyzed for every set of user defined inputs. Results of this study showed that TPB formation in a composite electrode was most effective when the electronic volume fraction is quite low, usually 15% or less and when the gas/current collector boundary contained highly intermixed gas and electronic conductor phase. Besides, sorbate transport always improves the formation of TPBs.

Computational fluid dynamics (CFD) is another useful method to apply the reaction mechanism on the macro-scale cathode systems. It uses numerical methods and algorithms to solve and analyze problems that involve fluid flows. Commercial CFD code FLUENT was usually used in SOFC modeling simulation. Autissier et al. [72] utilized CFD to predict current density, flow, temperature and concentration fields for a whole stack. Jeon [73] also utilized CFD method to simulate a two-dimensional model for anode-supported SOFC. And he found that the contribution of cathode overpotential was dominant at low current density.

3.3. Summary

The literature reviewed in this part has shown that the oxygen reduction mechanism in the cathode of an SOFC is complex. Although different experimental methods have been utilized to verify model results, as we will see below in Section 4, differences of opinion still exist among researchers. Several main debatable issues about SOFC cathode reaction mechanisms are summarized as below:

(1) Reaction intermediates: Different sub-reactions were offered by researchers for the same overall oxygen reduction reaction. Adsorbed oxygen atoms, O^- and O^-_2 were all possible to appear via one or more steps. The surface overpotential needs to be considered when there are chargeable intermediates during the reduction process. However, based on the present investigated

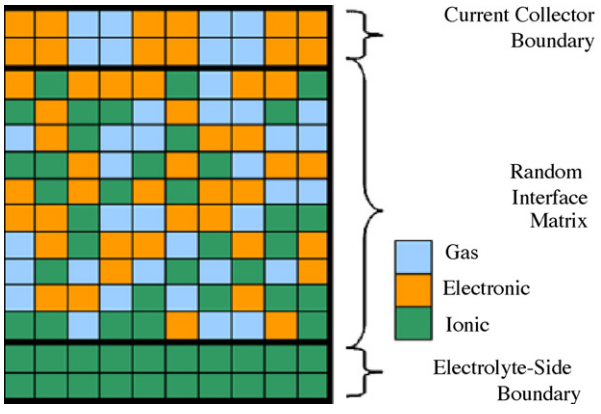

Fig. 13. Sample randomized monodispersed interface structure [71].

literature, it is still difficult to determine which intermediates actually exist in the reaction.

(2) Reaction region: Generally, the TPB region where cathode, electrolyte and gas connect together was supposed to be the main reaction region. However, due to the fact that the cathode material is a mixed ionic and electronic conductor, oxygen reduction also may occur at gas/cathode interface. Therefore, two charge-transfer pathways will co-exist and compete under different operation conditions.

(3) Rate limited steps: As stated before, the overall oxygen reduction can be divided into several sub-reactions according to the understandings of oxygen reduction mechanism. Besides the reduction reactions, oxygen diffusion is the other step for the cathode reaction process. Rate limited step determination under different conditions is important for optimizing the cathode and improving the cell efficiency.

(4) Geometry factors: Geometry factors such as porosity, tortuosity and TPB length are important for SOFC cathode modeling. They will affect the gas diffusion process and the cell performance. Due to the fact that the shape and the distribution of the pores inside SOFCs cathode are random, it is difficult to get an accurate simulation result compared to the real operating conditions. Some researchers applied a factor parameter to minimize the errors on ignoring the geometry effects. Most researchers used a computer to build up a random microstructure with some input parameters. An effective way is to get part of the microstructure information from the experimental method first, then use a computer program to simulate the entire cathode reaction process.

4. Experimental methods for model verification

Experimental results are usually applied to verify the conclusions of a cathode model. Improved electrochemical and new detection methods had been developed to make the analysis more reliable.

4.1. Traditional electrochemical methods

Electrochemical impedance spectroscopy (EIS) is used extensively to probe the electrochemical characteristics of SOFC electrodes. It offers useful information of the interface behavior. Anne et al. used EIS data to study the mechanism and kinetics of oxygen reduction reaction at a composite SOFC cathode which consisted of lanthanum strontium manganite in a 50 vol.% mixture with yttria-stabilized zirconia electrolyte [74].

Fig. 14 is the Nyquist plot of the EIS data and the equivalent circuit. The equivalent circuit included three R/CPE units in series with a fourth resistor and an inductor. Based on the authors' analysis, R_1 is the resistance between the reference electrode and the working electrode. R_2 and R_3, which originated from the high and mid frequency arcs and independent of O_2 partial pressure, are associated with the Pt/LSM and LSM/LSM-YSZ interfaces or with grain boundaries. R_4 shows a strong dependence on the oxygen partial pressure. As shown in Fig. 14, when the oxygen partial pressure is lower than 0.5 atm, besides the two semicircles at high and mid frequency, a third semicircle can be seen at low frequency. The authors claimed that R_4 is assigned to the charge-transfer resistance.

Baek et al. also applied the EIS method to study the mechanism of a new $Sm_{0.5}Sr_{0.5}CoO_{3-\delta}/Sm_{0.2}Ce_{0.5}O_{1.9}$ composite cathode [75]. Based on the experimental data, a three semicircle model was used to analyze the oxygen reduction process. The equivalent circuit is shown in Fig. 15. Similar to Anne's analysis results, the cathode included three resistances with three constant phase elements. The resistances were presented as $R_{c,HF}$, $R_{c,MF}$ and $R_{c,LF}$ which stand for high frequency, middle frequency and low frequency respectively. Baek explained the resistance at medium frequency as a result of the oxygen ion conduction. And the electrode resistance at low frequency was claimed for a non-charge transfer related to the gas phase diffusion of oxygen. The high frequency resistance represents the oxygen ion transfer at the cathode/electrolyte interface.

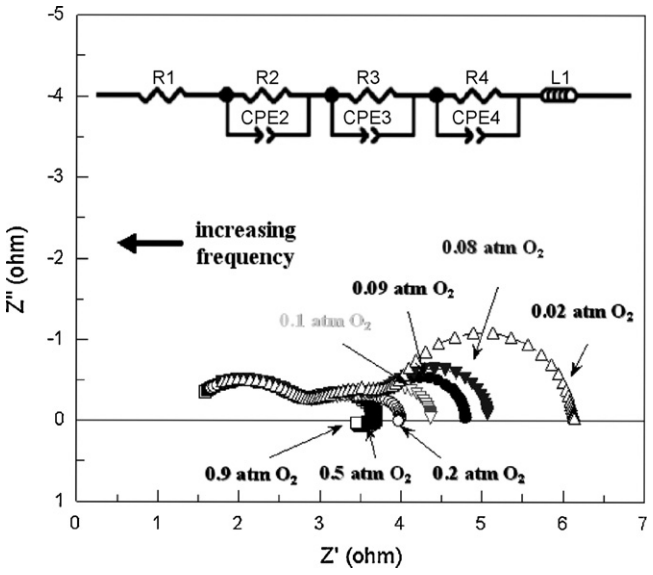

Fig. 14. Complex impedance spectra of LSM–YSZ composite cathode on YSZ disk at 800 °C at various O_2 partial pressures [74].

Baumann employed geometrically well-defined $La_{0.6}Sr_{0.4}Co_{0.8}Fe_{0.2}O_{3-\delta}$ micro-electrode to elucidate the individual resistive and capacitive processes of SOFCs cathode by means of impedance spectroscopy [76]. Electrochemical resistance associated with oxygen exchange at the cathode surface (R_s) had been observed at the low frequencies. And the resistive component of the middle frequency R_i corresponded to the transfer of oxide ions O^{2-} across the electrode/YSZ interface. Besides the high frequency resistance R_b was attributed mainly to the ohmic resistance of the electrolyte (Fig. 16).

Liu et al. analyzed the effects of the surface overpotential and temperature at LSCF/GDC electrode interface on YSZ by AC impedance [77]. In this work, relationship between surface overpotential and polarization resistance R_p, which is composed of the low frequency semicircle resistances, had been studied. As Fig. 17 shown, based on the experimental results, Liu claimed the resistance-overpotential curve obeys an exponential law:

$$\ln R_p = a + b\eta \tag{25}$$

Further, the potential step method was used to study the time dependence of the interfacial properties during polarization. Liu utilized this method to characterize the formation and spillover of oxygen vacancies over the LSM electrode [78]. In their experiments, the working electrode was first subjected to a −0.8 V potential with respect to the reference electrode until the current reached a stable value. Then the potential applied to the electrode was stepped to 0.4 V to eliminate the oxygen vacancies in the electrode. After the anodic current reached a steady-state value, the potential applied to the working electrode was then stepped back to −0.8 V and the current response was recorded as a function of time. The difference between the current relaxation results, as shown in Fig. 18, suggested that the oxygen reduction at the LSM/LSGM interface is primarily limited by the TPB reaction and LSM/gas interface reaction did not contribute significantly to the overall electrode reaction.

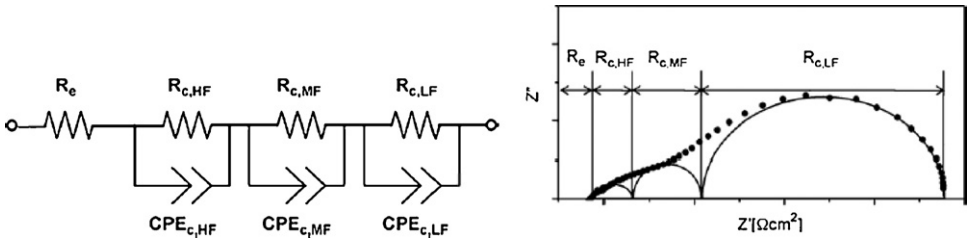

Fig. 15. Equivalent circuit model for $Sm_{0.5}Sr_{0.5}CoO_{3-\delta}/Sm_{0.2}Ce_{0.5}O_{1.9}$ composite cathode [75].

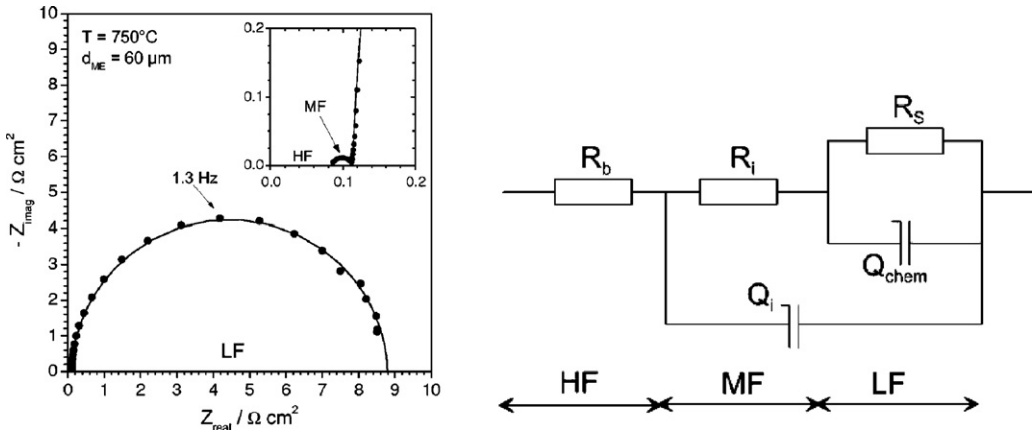

Fig. 16. Impedance spectrum and equivalent circuit of $La_{0.6}Sr_{0.4}Co_{0.8}Fe_{0.2}O_{3-\delta}$ micro-electrode [76].

Yi et al. [79] performed ac impedance, cyclic voltammetry and potential step experiments to investigate the oxygen vacancy formation and its contribution to the oxygen reduction. The total current was considered to be consisting of two parts which included i_{TPB} from the electrochemical reaction at the three-phase boundary and i_{2PB} from the oxygen reduction at the cathode/gas interface. The simulated results showed that the surface exchange process may play an important role in the cathode reaction process depending on P_{O_2} and step potential applied. Hence they hold the point that the cathodic polarization can be ascribed to the formation of oxygen vacancies. And the vacancies would propagate over the LSM surface since the bulk diffusion was considered very slow.

4.2. Improved and new methods

The traditional electrochemical methods, as illustrated above, are used widely for electrode reaction process investigation. However, there are some disadvantages for application of those methods. And recently researchers tried to improve the traditional method or use some new method to study the entire reaction process.

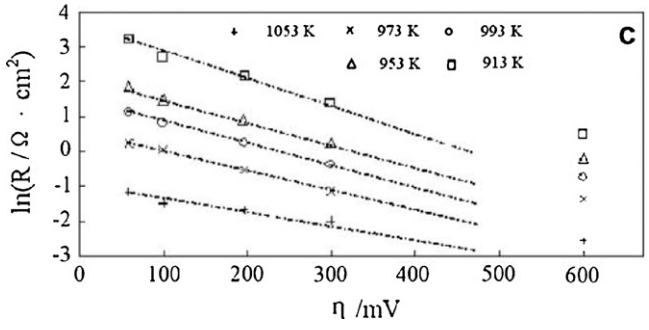

Fig. 17. Effect of overpotential on R_p at LSCF cathode–YSZ electrolyte interfaces [77].

The application of EIS has two limitations. A major factor limiting the usefulness of EIS data is overlap or dispersion in the frequency domain among physical processes governing electrode reactions, making them difficult to resolve entirely by time. Another factor is that different mechanistic models for a given reaction often predict very similar impedance response after the governing equations have been linearized. Adler et al. extended EIS to probe both linear and nonlinear response [80]. This technique involves the measurement of nonlinear second and high order voltage harmonics resulting from moderate-amplitude current perturbations. Nonlinear EIS (NLEIS) has three advantages compared to the traditional nonlinear measurements. Above all, it may better isolate the nonlinearities of specific physical processes. In the next place, NLEIS may offer improved measurement resolution of nonlinear behavior. Third, this technique can gather nonlinear information more efficiently. A symmetrical cell which consisted two porous $La_{0.8}Sr_{0.2}CoO_{3-\delta}$ cathode layers and one 250 μm thick Sm-doped ceria electrolyte had been investigated by NLEIS. They compared the measured results with those predicted results for oxygen adsorption kinetics. And they considered that the electrode operated by parallel surface and bulk paths where the concentration of mobile vacancies on the surface is much higher than in the bulk.

Vladikova et al. [81,82] applied differential impedance analysis (DIA), which provides both structural and parametric identification without preliminary consideration about the working model to investigate the cathode reaction. The secondary differential impedance analysis is performed by differentiating the local operating model (LOM) parameter estimates with respect to the frequency. The exponent parameters of CPE can be determined by the differential of LOM parameters.

Recently, in situ investigation of the cathode reaction process became a new focus for researchers. Backhaus-Ricoult et al. studied an LSM cathode with different overpotentials in situ by photoelectron microscopy [83]. Fig. 19 is the XPS spectra images of different elements at the interface of LSM/YSZ. They claimed the strong enrichment of the electrolyte surface in Mn^{2+} provided high

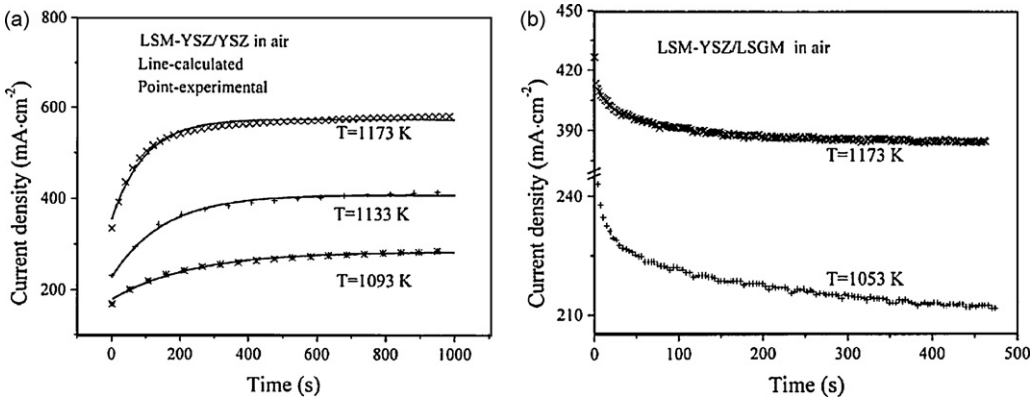

Fig. 18. Current relaxation after the working electrode was stepped at −0.8 V [78].

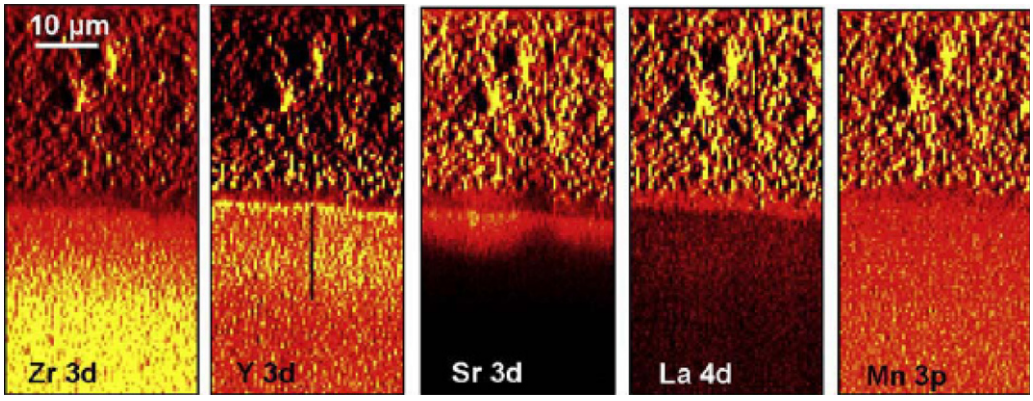

Fig. 19. Spectro-images of Zr 3d, Y 3d, Sr 3d, La 4d and Mn 3p peaks in the triple phase boundary area at bias −0.6 V. [83].

electronic conductivity and promoted the direct incorporation of oxygen from the gas into the electrolyte by

$$\frac{1}{2}O_2(gas) + 2Mn''_{cat} + V_{\ddot{O}} = 2Mn'_{cat} + O_O^x \quad (26)$$

4.3. Summary

Using experimental methods to prove the simulation results of the cathode modeling is necessary for the cathode reaction investigation. Both traditional electrochemical methods and some new utilized methods have been summarized in this part. As an effective tool on studying the interface reactions, traditional electrochemical methods played an important role in the experimental research field. And some researchers applied improved analysis methods to make the analyzed result more reliable. At the same time, modern surface analysis technologies have been widely utilized on the in situ study. However, the arguable issue about the intermediates type has not been solved yet.

5. Concluding remarks and future work

In last decades, tremendous amount of efforts have been devoted to modeling the SOFC cathode reaction process and the experimental verifications. However, due to the fact that the reaction system and conditions are very complex, no universal model has been developed and had been completely verified. A lot of problems and debates still exist in this field so far. Here, we try to summarize some general conclusions of the SOFC cathode modeling efforts and the give our opinion on the needs for future studies on this topic.

First, for MIEC material, most researchers held the point that there are two pathways for the mass transport. And they agreed that the intermediates should appear during the transport process. However, we do not know the type of the intermediates. Some claimed that the intermediates should be neutral species and so they treated the oxygen reduction process as a pure chemical process. Others believed there are different kinds of charged intermediates. They treated the oxygen reduction as an electrochemical process and surface overpotential has been involved in their simulation. Although some researchers offered the theoretical and experimental proof of the charged intermediates on metal electrode, we do not know with certainly the existence of charged intermediates for MIEC.

Through this review, it can be also seen that how we deal with the geometry parameter affects in the simulation. The images of electrode/electrolyte interface were applied to get the TPB length. Some computer-based methods also have been utilized to simulate the microstructure of the porous electrode. However, for those complex diffusion and reaction system, it is still difficult to get accurate simulation results.

Finally, the experimental methods which were applied to SOFC cathode mechanism studies were reviewed. The electrochemical impedance spectroscopy method is the most important method for studying the interface behavior. There is not just one equivalent circuit model that can be used to explain the EIS data. Improved methods, such as nonlinear EIS and differential impedance analysis can solve this problem. Some other electrochemical methods also have been utilized to investigate the cathode polarization phenomena. Recently, in situ methods using surface analysis technology have become a research focus. Compared to the traditional

electrochemical experimental methods, it can offer some direct information and it is more conclusions.

One particularly neglected issue is the effects of P_{O_2} at electrode/electrolyte interface on oxygen reduction. Based on the knowledge of the nonstoichiometry perovskite materials, the surface exchange and bulk diffusion coefficients will change with the oxygen partial pressure change. Due to the fact that reaction rate at the TPB being assumed fast, the oxygen concentration of the gas should be low in this region. On the other hand, P_{O_2} value at the electrode/electrolyte interface also will be affected by the cathode polarization. Investigation on the relationship among the kinetic parameters of the cathode material, electrode/electrolyte interface P_{O_2} and the polarization potential is important to determine the rate limited step for the entire reaction process.

Besides, as shown in this review, some researchers tried to simplify the oxygen pathways while some others considered all the possibilities when they set up the cathode models. Too many simplifications may make the model apart from the reality. At the same time, it is too difficult to get the simulation results with considering all the possible reactions. Therefore, it is necessary to set up a model which can consider the most important oxygen transport pathways and be resolvable, at least numerically.

Moreover, improving the experimental investigation methods is also very important. It includes developing advanced detective techniques and accurate mathematical analysis methods. Recently some surface analysis techniques such as XPS, SEM had been applied for in situ investigation of SOFCs cathode reactions. However, limited by temperature and vacuum requirements of those equipments, the tests still cannot be done under the real SOFC operation conditions. On the other hand, most of the electrochemical experimental results need to be analyzed by mathematical methods. Therefore, it is necessary to improve the analysis to get more reasonable conclusions. For example, the diffusion solution used for electrical conductivity relaxation testing is deduced by assuming that oxygen vacancy concentration inside the sample is a constant. However, it is well known that under different oxygen partial pressure the vacancy concentration varies. So the parameters fitted by the solution are not the accurate real values.

Acknowledgements

This technical effort was performed in support of the National Energy Technology Laboratory's on-going research in West Virginia University under contract #DE-AC26-04NT41817. The assistance of Richard Pineault and David Ruehl from NETL in Morgantown, WV and fruitful discussion with Dr. Kirk Gerdes are highly appreciated. The authors also would like to gratefully acknowledge for Mingyang Gong's (Ph.D. student, WVU) help and suggestions on this work.

References

[1] N.Q. Minh, Solid State Ionics 174 (1–4) (2004) 271–277.
[2] J.C. Ruiz-Morales, J. Canales-Vazquez, C. Savaniu, D. Marrero-Lopez, W. Zhou, J.T.S. Irvine, Nature 439 (2) (2006) 568–571.
[3] Y.-H. Huang, R.I. Dass, Z.-L. Xing, J.B. Goodenough, Science 312 (2006) 254–257.
[4] Z. Zhan, S.A. Barnett, Science 308 (2005) 844–847.
[5] S.P.S. Badwal, K. Foger, Ceramics International 22 (3) (1996) 257–265.
[6] H. Zhao, F. Mauvy, C. Lalanne, J.-M. Bassat, S. Fourcade, J.-C. Grenier, Solid State Ionics 179 (35–36) (2008) 2000–2005.
[7] A. Princivalle, E. Djurado, Solid State Ionics 179 (33–34) (2008) 1921–1928.
[8] Fuel Cell Handbook, seventh edition, EG&G Technical Services, Inc., 2004, Chapter 7-P5.
[9] F. Tietz, A. Mai, S. Detlev, Solid State Ionics 179 (27–32) (2008) 1509–1515.
[10] J. Mizusaki, N. Mori, H. Takai, Y. Yonemura, H. Minamiue, H. Tagawa, M. Dokiya, H. Inaba, K. Naraya, T. Sasamoto, T. Hashimoto, Solid State Ionics 129 (1–4) (2000) 163–177.
[11] T. Tsai, S.A. Barnett, Solid State Ionics 93 (3–4) (1997) 207–217.
[12] R.A. De Souza, J.A. Kilner, J.F. Walker, Materials Letters 43 (1–2) (2000) 43–52.
[13] P. Leone, M. Santarelli, P. Asinari, M. Calì, R. Borchiellini, Journal of Power Sources 177 (1) (2008) 111–122.
[14] V.V. Srdić, R.P. Omorjan, S. Johannes, Materials Science and Engineering B 116 (2) (2005) 119–124.
[15] C. Xia, W. Rauch, F. Chen, L. Meilin, Solid State Ionics 149 (1–2) (2002) 11–19.
[16] H. Fukunaga, M. Koyama, N. Takahashi, C. Wen, K. Yamada, Solid State Ionics 132 (3–4) (2000) 279–285.
[17] H. Lv, Y.-j. Wu, B. Huang, B.-y. Zhao, H. Ke-ao, Solid State Ionics 177 (9–10) (2006) 901–906.
[18] X. Ding, C. Cui, X. Du, G. Lucun, Journal of Alloys and Compounds 475 (1–2) (2009) 418–421.
[19] W. Zhou, R. Ran, Z. Shao, Journal of Power Sources 192 (2) (2009) 231–246.
[20] P.G. Bruce (Ed.), Solid State Electrochemistry, Cambridge University Press, Scotland, 1995, p. 163.
[21] F.W. Poulsen, Solid State Ionics 129 (1–4) (2000) 145–162.
[22] H. Kamata, Y. Yonemura, J. Mizusaki, H. Tagawa, K. Naraya, T. Sasamoto, Journal of Physical Chemistry and Solid 56 (7) (1995) 943–950.
[23] J. Mizusaki, Y. Yonemura, H. Kamata, K. Ohyama, N. Mori, H. Takai, H. Tagawa, M. Dokiya, K. Naraya, T. Sasamoto, H. Inaba, T. Hashimoto, Solid State Ionics 132 (3–4) (2000) 167–180.
[24] M. Oishi, K. Yashiro, K. Sato, J. Mizusaki, K. Tatsuya, Journal of Solid State Chemistry 181 (2008) 3177–3184.
[25] W. Huang, S. Gopalan, P. Uday, Journal of Power Sources 173 (2) (2007) 887–890.
[26] A. Endo, M. Ihara, H. Komiyama, Y. Koichi, Solid State Ionics 86–88 (1996) 1191–1195.
[27] R.J. Chater, S. Carter, J.A. Kilner, B.C.H. Steele, Solid State Ionics 53–56 (2) (1992) 859–867.
[28] N. Sakai, K. Yamaji, T. Horita, H. Kishimoto, M.E. Brito, H. Yokokawa, Y. Uchimoto, Applied Surface Science 252 (19) (2006) 7045–7047.
[29] I. Yasuda, H. Tomoji, Journal of Electrochemical Society 141 (5) (1994) 1268–1273.
[30] R.A. De Souza, J.A. Kilner, Solid State Ionics 106 (3–4) (1998) 175–187.
[31] R.A. De Souza, J.A. Kilner, Solid State Ionics 126 (1–2) (1999) 153–161.
[32] J.A. Kilner, R.A. De Souza, I.C. Fullarton, Solid State Ionics 86–88 (2) (1996) 703–709.
[33] I. Yasuda, K. Ogasawara, M. Hishinuma, T. Kawada, M. Dokiya, Solid State Ionics 86–88 (2) (1996) 1197–1201.
[34] E.S. Raj, J.A. Kilner, T.S. John, Solid State Ionics 177 (19–25) (2006) 1747–1752.
[35] C.-R. Song, H.-I. Yoo, Solid State Ionics 120 (1–4) (1999) 141–153.
[36] L.M. van der Haar, M.W. den Otter, M. Morskate, H.J.M. Bouwmeester, H. Verweij, Journal of the Electrochemical Society 149 (3) (2002) 41–46.
[37] J. Crank, The Mathematics of Diffusion, Oxford University Press, 1975 (Chapters 3–5, pp. 28–88).
[38] L. Chen, C.L. Chen, A.J. Jacobson, IEEE Transactions on Applied Superconductivity 13 (2) (2003) 2882–2885.
[39] J.A. Lane, J.A. Kilner, Solid State Ionics 136–137 (2) (2000) 997–1001.
[40] M.W. den Otter, H.J.M. Bouwmeester, B.A. Boukamp, H. VerweijReactor, Journal of the Electrochemical Society 148 (2) (2001) 1–6.
[41] I. Yasuda, H. Masakazu, Journal of Solid State Chemistry 123 (2) (1996) 382–390.
[42] R.J. Bell, G.J. Millar, D. John, Solid State Ionics 131 (3–4) (2000) 211–220.
[43] C.C. Kan, H.H. Kan, F.M. Van Assche IV, E.N. Armstrong, E.D. Wachsman, Journal of Electrochemistry Society 155 (10) (2008) B985–B993.
[44] C.C. Kan, E.D. Wachsman, Journal of Electrochemistry Society 156 (6) (2009) B695–B702.
[45] K. Kammer, Solid State Ionics 177 (11–12) (2006) 1047–1051.
[46] J.M. Serra, B. Hans-Peter, Journal of Power Sources 172 (2) (2007) 768–774.
[47] L. Zhong, J. Luo, K. Chuang, Chinese Journal of Chemical Engineering 15 (3) (2007) 305–308.
[48] S.B. Adler, J.A. Lane, B.C.H. Steele, Journal of Electrochemistry Society 143 (11) (1996) 3554–3564.
[49] M. Liu, J. Winnick, Journal of Electrochemistry Society 144 (5) (1997) 1881–1883.
[50] S.B. Adler, Solid State Ionics 135 (1–4) (2000) 603–612.
[51] A.M. Svensson, S. Sunde, K. Nisancioglu, Solid State Ionics 86–88 (2) (1996) 1211–1216.
[52] A.M. Svensson, S. Sunde, K. Nisancioglu, Journal of the Electrochemical Society 144 (8) (1997) 2719–2732.
[53] G.W. Coffey, L.R. Pederson, Peter C. Rieke, Journal of The Electrochemical Society 150 (8) (2003) 1139–1151.
[54] G. Kopasakis, T. Brinson, S. Credle, M. Xu, NASA/TM—2006-214104, GT2006-91247.
[55] Meilin Liu, Winnick Jack, Solid State Ionics 118 (1–2) (1999) 11–21.
[56] F.H. van Heuveln, H.J.M. Bouwmeester, Journal of Electrochemical Society 144 (1) (1997) 135–140.
[57] A. Mitterdorfer, Identification of the oxygen reduction at cathodes of solid oxide fuel cells, Ph.D. Dissertation, Swiss Federal Institute of Technology, 1997.
[58] S.H. Chan, X.J. Chen, K.A. Khor, Journal of The Electrochemical Society 151 (1) (2004) A164–A172.
[59] B. Yildiz, G.J. Ia O', Y. Shao-Horn, Preparative Paper—American Chemical Society, Division on Fuel Chemistry 2 (2004) 49.
[60] J.-H. Wang, M. Liu, M.C. Lin, Solid State Ionics 177 (9–10) (2006) 939–947.
[61] Fleig Jurgen, Physical Chemistry and Chemical Physics 7 (2005) 2027–2037.
[62] F.S. Baumann, J. Maier, J. Fleig, Solid State Ionics 179 (21–26) (2008) 1198–1204.
[63] F.S. Baumann, J. Fleig, H.-U. Habermeier, M. Joachim, Solid State Ionics 177 (11–12) (2006) 1071–1081.

[64] D.S. Mebane, Y. Liu, L. Meilin, Journal of The Electrochemical Society 154 (5) (2007) A421–A426.
[65] D.S. Mebane, L. Meilin, Journal of Solid State Electrochemistry 10 (2006) 575–580.
[66] V.M. Janardhanan, V. Heuveline, O. Deutschmann, Journal of Power Sources 178 (1) (2008) 368–372.
[67] Ali Abbaspour, K. Nandakumar, Jingli Luo, Karl T. Chuang, Journal of Power Sources 161 (2) (2006) 965–970.
[68] J. Deseure, L. Dessemond, Y. Bultel, S. Elisabeth, Journal of the European Ceramic Society 25 (12) (2005) 2673–2676.
[69] J. Deseure, Y. Bultel, L. Dessemond, E. Siebert, Electrochimica Acta 50 (2005) 2037–2046.
[70] Ji Yan, Yuan Kun, J.N. Chung, Journal of Power Sources 165 (2007) 774–785.
[71] Andrew S. Martinez, Brouwer Jacob, Electrochimica Acta 53 (10) (2008) 3597–3609.
[72] N. Autissier, D. Larrain, J. Van herle, D. Favrat, Journal of Power Sources 131 (1–2) (2004) 313–319.
[73] D.H. Jeon, Electrochimica Acta 54 (10) (2009) 2727–2736.
[74] A.C. Co, S.J. Xia, V.I. Birss, Journal of The Electrochemical Society 152 (3) (2005) A570–A576.
[75] S.-W. Baek, J. Bae, Y.-S. Yoo, Journal of Power Sources 193 (2) (2009) 431–440.
[76] F.S. Baumann, J. Fleig, G. Cristiani, B. Stuhlhofer, H.-U. Habermeier, J. Maiera, Journal of The Electrochemical Society 154 (9) (2007) B931–B941.
[77] Liu Shiming, Suo Jinping, Xiao. Jianzhong, International Journal of Hydrogen Energy 33 (2008) 6322–6326.
[78] S. Wang, X. Lu, M. Liu, Journal of Solid State Electrochemistry 6 (2002) 384–390.
[79] Y. Jiang, S. Wang, Y. Zhang, J. Yan, W. Li, Journal of Electrochemistry Society 145 (2) (1998) 373–378.
[80] J.R. Wilson, D.T. Schwartz, S.B. Adler, Electrochimica Acta 51 (8–9) (2006) 1389–1402.
[81] D.E. Vladikova, Z.B. Stoynov, A. Barbucci, M. Viviani, P. Carpanese, J.A. Kilner, S.J. Skinner, R. Rudkin, Electrochimica Acta 53 (25) (2008) 7491–7499.
[82] D. Vladikova, Z. Stoynov, Journal of Electroanalytical Chemistry 572 (2) (2004) 377–387.
[83] M. Backhaus-Ricoult, K. Adib, St.T. Clair, B. Luerssen, L. Gregoratti, A. Barinov, Solid State Ionics 179 (21–26) (2008) 891–895.